Available online at www.sciencedirect.com
SCIENCE DIRECT
Neuroscience Letters 404 (2006) 270–275
Neuroscience Letters
www.elsevier.com/locate/neulet

En block C-terminal charge cluster reversals in prestin (SLC26A5): Effects on voltage-dependent electromechanical activity

Jun-Ping Bai [b], Dhasakumar Navaratnam [a], Haresha Samaranayake [a], Joseph Santos-Sacchi [b,*]

[a] *Neurology and Neurobiology, Yale University School of Medicine, BML 246, 333 Cedar Street, New Haven, CT 06510, USA*
[b] *Otolaryngology Neurobiology, and Cellular and Molecular Physiology, Yale University School of Medicine, BML 246, 333 Cedar Street, New Haven, CT 06510, USA*

Received 18 August 2005; received in revised form 8 May 2006; accepted 9 May 2006

Abstract

Prestin, the transmembrane motor protein is a novel protein underlying the motility of the outer hair cells. Nonlinear capacitance (NLC) or gating charge current, which can be observed in both auditory and transfected non-auditory cells, is the electrical signature of prestin's electromechanical activity. To test the functional role of the C-terminus of prestin, several charged residue clusters were reversed en-block by site-directed mutagenesis. They are D/E to K at 516, 518, 522, 524, 527, 528 and 531 (*cluster a*); R/K to D at 571, 572, 573, 576, 577 and 580 (*cluster b*); R to D at 571; and E/D to K at 608, 609, 610, 611, 612 and 613 (*cluster c*). These constructs were transfected into Chinese hamster ovary cells (CHO) and NLC recordings were performed to evaluate the effects of these charge substitutions. All of the mutants showed NLC. Charge *cluster a* reversal significantly reduced the maximum charge movement (Q_{max}). All but one mutation (charge *cluster c* reversal) shifted V_h, indicative of the operating voltage range, in the depolarizing direction. None of the mutations affected unitary charge movement (z). These data suggest that the C-terminus of prestin lies outside the membrane voltage field, and may play an important role in controlling the operating voltage range through control of the protein's conformational energy profile via allosteric means.

Keywords: Capacitance; Outer hair cell; Prestin; SLC26

Two types of receptor cells populate the mammalian organ of Corti, the inner hair cell (IHC) and the outer hair cell (OHC). IHCs serve only as sensory receptors by transducing basilar membrane vibrations into electrical signals. However, OHCs function both as receptors and effectors, possessing both electro-mechanical and mechano-electrical activities, thereby enabling amplification of the auditory stimulus to the IHCs [2,5,21]. Voltage-dependent mechanical activity of the OHC is detectable by whole-cell patch clamp recording as a nonlinear capacitance (NLC), or equivalently, a gating charge current [3,25]. Recently, the motor protein, prestin, which resides in the OHC lateral membrane [4], was found to underlie OHC electro-mechanical activity and mammalian cochlear amplification [12,31,24]. Transfection of the gene into non-auditory cells results in electro-mechanical characteristics similar to that observed in the native outer hair cell [15,26,31]. Topology studies of this 744 amino acid protein, a member of the anion transporter family SLC26, show that its C- and N-termini reside within the cytoplasm [6,15,16,18,30]. Interestingly, intracellular chloride was found to play a key role in influencing NLC in both OHCs and prestin-transfected cells, but whether chloride itself is an intrinsic voltage sensor or an allosteric modulator is still debated [18,20]. We have found that removal of intracellular chloride by substitution with other anions causes shifts in prestin's operating voltage range, in addition to altering the protein's nonlinear charge transfer or NLC, indicating that anions modulate energy barriers controlling prestin's conformational state [20,27]. Additionally, we recently observed prestin–prestin interactions via their intracellular termini [17]. Such results may indicate that charged residues within prestin may interact with intracellular anions or influence interactions with other proteins. Many charged residues within the putative transmembrane regions of prestin have been manipulated [18]; however, little data are available on the role played by charged residues found within the cytoplasmic termini, structures which are unlikely to house the molecule's voltage sensor. Here we evaluate the effects of several C-terminal charge cluster reversals on prestin's electromechanical activity in order to gauge

* Corresponding author. Tel.: +1 203 785 5407; fax: +1 203 737 2502.
E-mail address: joseph.santos-sacchi@yale.edu (J. Santos-Sacchi).

0304-3940/$ – see front matter © 2006 Elsevier Ireland Ltd. All rights reserved.
doi:10.1016/j.neulet.2006.05.062

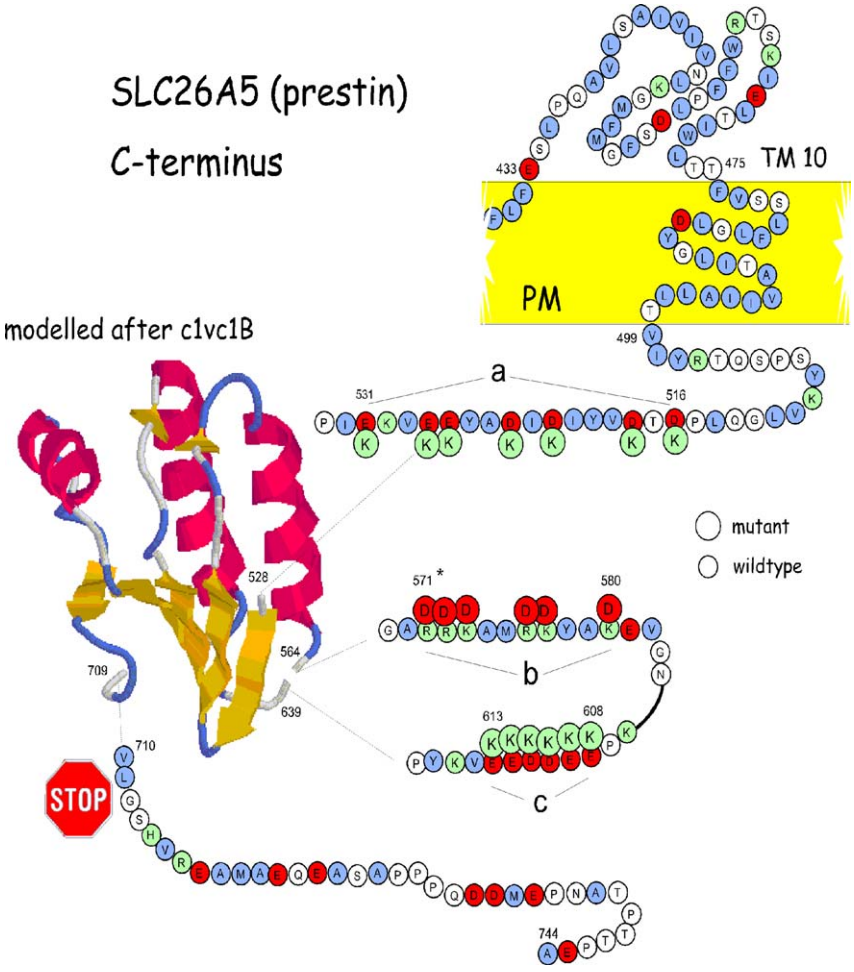

Fig. 1. C-terminal cartoon of gerbil prestin. Indicated are the charged clusters (a–c) which were mutated to residues of opposite polarity (large circles). The final transmembrane domain from the topology model of Navaratnam et al. [18] is shown along with the intracellular residues that were not captured in the model based on 3D structure of the sequence of c1vc1B, the putative anti-sigma factor antagonist tm1442. The model gives an excellent prediction of prestin's C-terminal structure, but nearly all of the charged clusters we mutated reside in regions with no clear secondary structure. The residues 569–617 though present in prestin, are absent in c1vc1B. Parameters of the model fit: 19% i.d., 100% precision and a 6.4e-7 E value. The stop indicates the position (709) of the C-terminal truncation that results in a loss in NLC [18].

the C-terminal contribution to allosteric modulation of motor function.

The gerbil prestin sequence [31] was submitted to Quick Phyre (http://www.sbg.bio.ic.ac.uk/~phyre/) fold facility for 3D structural modeling and the C-terminal region of prestin was best fit with the structure encoded by the putative anti-sigma factor antagonist tm1442 (PDBcode: 1vc1_B; characteristic of the STAS domain [1]), at 19% i.d., 100% precision and a 6.4e-7 E value. The structure is shown in Fig. 1 along with noted mutations that we made in the prestin sequence. Though the STAS domain stretches from 525–711, the model is more limited.

We changed two negatively charged clusters to positive (residues 516–531 and 608–613; designated as charge *clusters a* and *c*, respectively), and changed one positively charged cluster to negative (571–580; *cluster b*). Additionally, a single site charge substitution was made at residue 571, denoted by "*" in Fig. 1. Charged amino acids were mutated en-block using the megaprimer PCR amplification method. Amplification by PCR was done using Hi-Fidelity DNA polymerase (Roche). The parameters were: 10 cycles of 94 °C for 40 s, 55 °C for 2 min, 68 °C for 6 min; 30 cycles of 94 °C for 40 s, 55 °C for 2 min, 68 °C for 6 min with 20 s extension for every cycle. A clone of gerbil prestin served as the template (courtesy of Zheng et al. [31]). Amplified products were purified, and ligated into PCDNA 3.1. Each of the clones generated were sequenced to exclude the possibility of PCR generated errors. Transient co-transfection with EGFP into Chinese hamster ovary cells (CHO) was achieved with Lipofectamine in accordance with the manufacturer's recommendations. The ratio of prestin to EGFP plasmid (2:1) was kept constant in all the experimental groups. All cells showing NLC were included in our analyses.

Cells were recorded by whole-cell patch clamp configuration at room temperature using an Axon 200A amplifier (Axon Instruments, CA, USA), as described previously [25]. Expression levels, as evidenced by NLC measures, were stable from 24–72 h after transfection in control group. All statistical analyses of the mutants were performed at the 48 h time period following transfection. The bath solution contained (in mM): TEA 20, CsCl 20, $CoCl_2$ 2, $MgCl_2$ 1.47, Hepes 10, NaCl 99.2, $CaCl_2{\cdot}2H_2O$ 2, pH 7.2, and the pipette solution contained (in

mM): CsCl 140, EGTA 10, $MgCl_2$ 2, Hepes 10, pH 7.2. These conditions ensured that prestin-chloride interactions were maximal [18,20]. Osmolarity was adjusted to 300 ± 2 mOsm with dextrose. Command delivery and data collections were carried out with a Windows-based whole-cell voltage clamp program, jClamp (Scisoft, CT, USA), using a NI PCI 6052E interface (National Instruments Co., USA).

Capacitance was evaluated with a continuous high-resolution 2-sine wave technique fully described elsewhere [22,25]. Capacitance data were fitted to the first derivative of a two-state Boltzmann function:

$$C_m = Q_{max}\frac{ze}{kT}\frac{b}{(1+b)^2} + C_{lin} \quad (1)$$

where

$$b = \exp\left(\frac{-ze(V_m - V_h)}{kT}\right)$$

Q_{max} is the maximum nonlinear charge transfer, V_h the voltage at peak capacitance or half-maximal nonlinear charge transfer, V_m the membrane potential, C_{lin} linear capacitance, z the valence (a metric of voltage sensitivity), e the electron charge, k the Boltzmann's constant and T the absolute temperature. Q_{max} is reported as Q_{sp} the specific charge density, i.e. total charge moved normalized to linear capacitance. A students t-test was used to evaluate the effects of mutations on the different parameters of NLC.

FACS analysis of the different mutants and prestin were done to determine levels of surface expression exclusively [17]. Two antibodies to prestin peptides (aa 274–290 and 359–375) that we model to lie on the outer surface of the membrane were used to live stain transfected CHO cells [17]. Staining was performed as previously described except that the secondary antibody used was an Alexa 488 labeled goat anti-rabbit antibody. There was good concordance between the two antibodies used to separately stain transfected cells, results that internally validated our data (see Fig. 4). We have previously established that prestin surface expression in CHO cells were unchanged between 24–72 h after transfection by both FACS analysis and measurement of NLC [17]. The percentage of cells expressing prestin on its surface and the magnitude in NLC in CHO cells are similar to that obtained by other investigators [17,18].

Fig. 1 depicts the structural features of prestin's C-terminus. Large circles indicate the charge reversals that were made and confirmed by sequencing. All charge substitution mutants displayed NLC, and did not affect unitary charge movement z. Q_{max}, was significantly different only with mutation of residues 516–531 (charge *cluster a*), which reduced Q_{max}. Fig. 2 shows an example of a NLC capacitance function obtained from this mutation and a control cell. For presentation purposes, we averaged fitted Boltzmann parameters, presented in Table 1, and constructed average NLC functions of each mutation based on their average values (Fig. 3). The mutation of *cluster a* had a significant decrease of Q_{max}, but unitary charge movement (z) remained normal, indicating that the mutated protein's voltage sensor remained unaltered, and only the number of functional proteins decreased. We confirmed that the levels of prestin surface expression in this (and other) mutant(s) were similar to

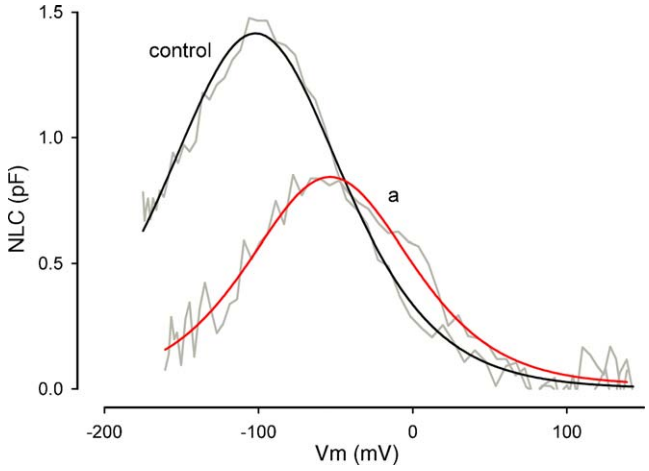

Fig. 2. NLC traces from prestin transfected CHO cells. CHO cells were transfected with constructs containing normal prestin (control) or the reversal of charge cluster a as indicated in Fig. 1. The solid traces are fitted curves. V_h of the reversal mutation shifts in the depolarizing direction along the voltage axis, and Q_{max} significantly decreases.

Table 1
Average fitted Boltzmann parameters

	Q_{sp} (fC/pF) ± S.E.	z ± S.E.	V_h (mV) ± S.E.
Control (n = 15)	6.15 ± 0.71	0.58 ± 0.03	−99.85 ± 2.51
Cluster a (n = 5)	2.90 ± 0.58	0.53 ± 0.04	−57.41 ± 5.51
Cluster b (n = 6)	6.23 ± 1.50	0.52 ± 0.04	−67.93 ± 1.73
Cluster c (n = 5)	5.10 ± 0.38	0.71 ± 0.01	−108.20 ± 6.45
Residue 571 (n = 7)	4.86 ± 0.63	0.65 ± 0.05	−90.19 ± 0.97

controls by FACS analysis (Fig. 4). z (and Q_{max}) remained stable in the other mutations too, confirming that these residues, as expected, do not serve as charge carriers through the membrane. Some substitutions significantly affected V_h, with opposite charge substitutions changing V_h in the same depolarizing direction. For example, a change of negative charge in *cluster a* to

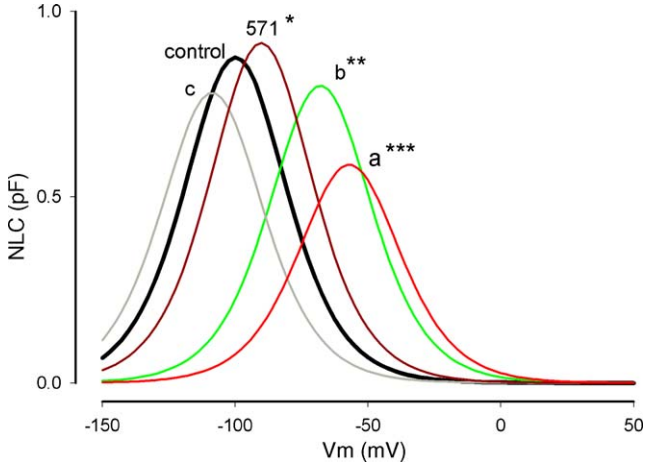

Fig. 3. C-terminal charge reversals predominately alter prestin's operating voltage range. For visual clarity, we averaged fitted parameters from each mutation, presented in Table 1, and constructed NLC functions of each based on their average values. Traces from each mutation are indicated as a, b, c and 571, and show some significant differences from control NLC, namely, for V_h and Q_{sp} ($^{*}P_{V_h} < 0.05$; $^{**}P_{V_h} < 0.05$; $^{***}P_{V_h} < 0.05$; $P_{Q_{sp}} < 0.05$, respectively. The trace from control cells is the heavy black line.

positive, and a change in positive charge in *cluster b* to negative resulted in a depolarizing shift in V_h to -57.41 ± 5.51 ($n = 5$) and -67.93 ± 1.73 mV ($n = 6$), respectively. These effects on prestin activity are likely due to changes in the steady state energy profile of prestin, i.e. an allosteric effect possibly through interference with interacting proteins or anions (see discussion). Interestingly, mutation of charge *cluster c* within the most distal charged cluster, showed little difference from controls. Finally, the single charge substitution at residue 571 showed only minor changes.

The topology of prestin (SLC26A5) has received much attention, as has that of the other family members of SLC26 [6,13–19,30]. Initial efforts indicated that the protein consists of 12 transmembrane domains (TM), with both C- and N-terminal regions residing intracellularly [6,15,16,18,29,30]. Though the location of these termini are fairly certain, various prediction programs provide a confusing profile of TM domains. Even so, epitope tagging and the putative location of reactive residues have narrowed our view. One of the popular maps places two N-glycosylation sites on the second extracellular loop [16], but we have since observed that this site may not reside extracellularly, but instead intracellularly [17]. Though our new model flips the protein within the plane of the membrane, while conserving the

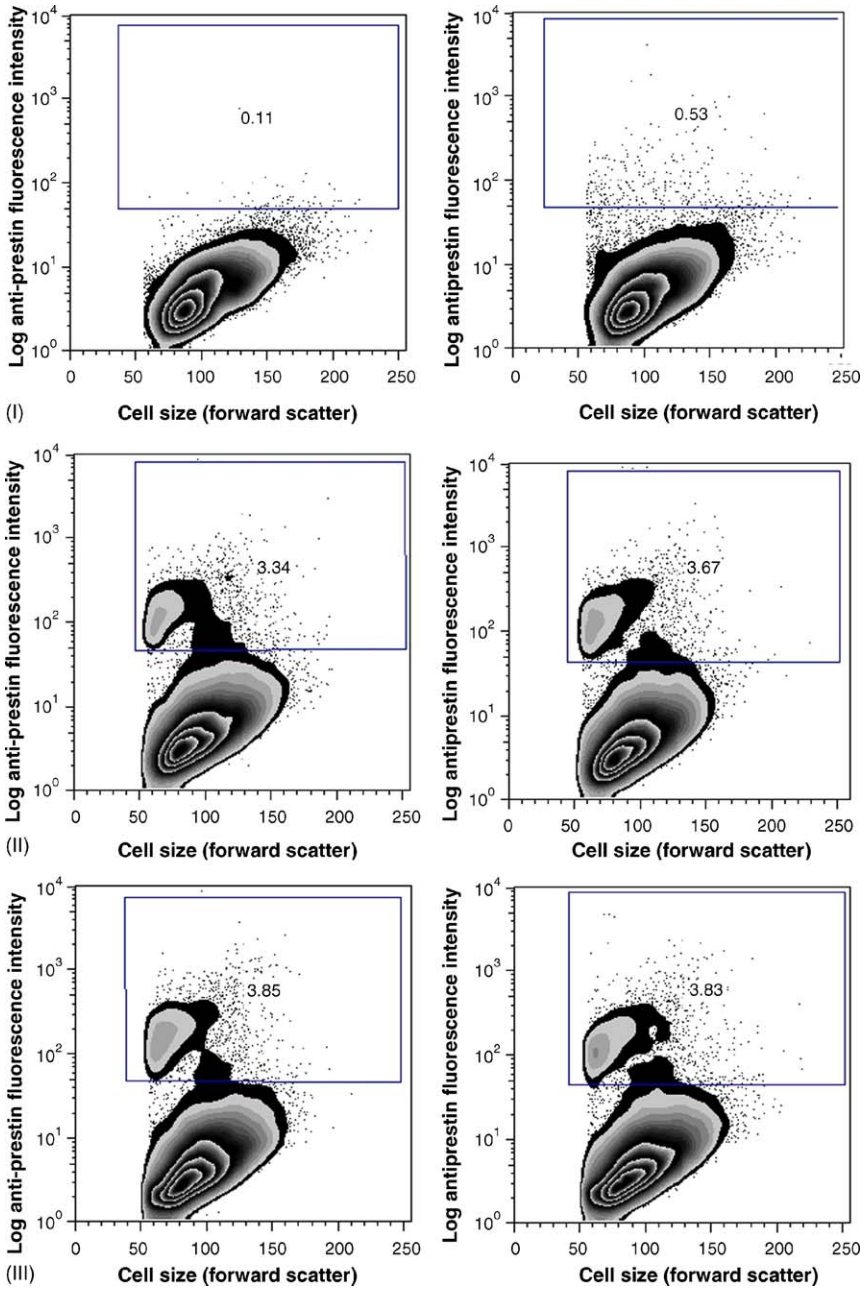

Fig. 4. Surface expression of cells transfected with normal prestin and mutant prestin were similar. Shown above are FACS plots of cells transfected with empty vector (I), normal prestin (II), charge cluster reversal a (III), charge cluster reversal b (IV) and charge cluster reversal c (V). The cells were live-stained with two antibodies against two peptides that we model to lie on the outer surface of the cell [18]. The percentage of cells with prestin surface expression (boxed area) reflecting efficiencies of transfection (inset) varied from 3.5 to 8.0% and are in line with results obtained by other groups (Oliver and Zheng, personal communication, see also [18]). The intensities of fluorescence between the different groups were similar confirming similar levels of surface expression.

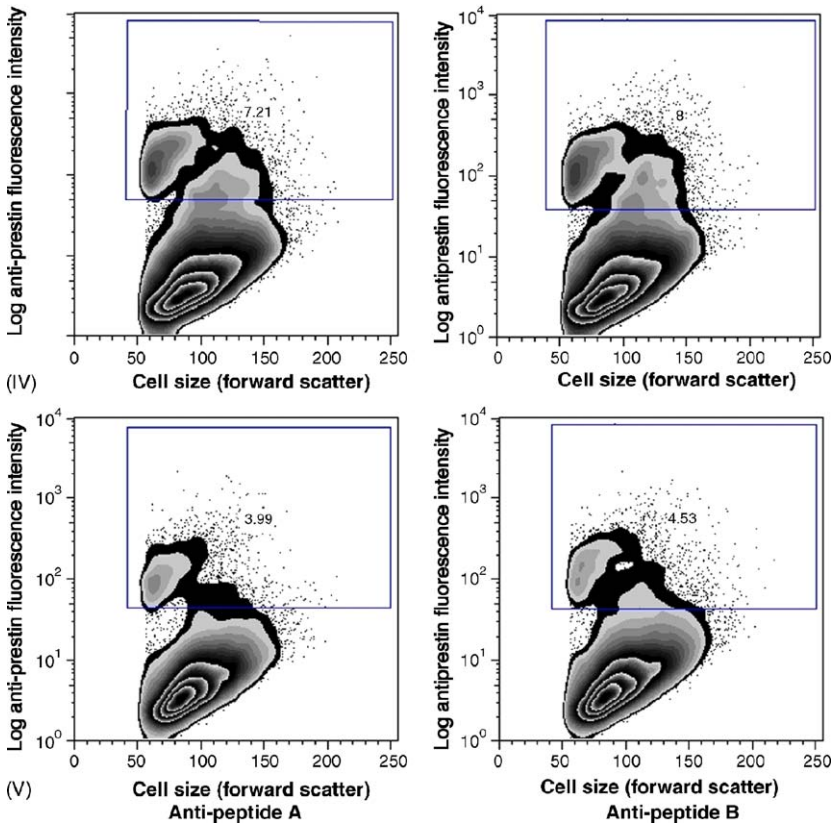

Fig. 4. (*Continued*).

intracellular termini and reversing the resident milieu of the non membrane bound loops, it maintains the intracellular location of a cGMP phosphorylation site proposed by Dallos and coworkers [6]; their modified model required a reentrant loop to intracellularly expose their previously predicted extracellular location of the site. Our model predicts simple TM transits. Clearly, the controversy over prestin's membrane topology indicates a complex interaction with the plasma membrane, which structural studies must finally divulge.

More germane to the present work, despite the seemingly clear localization of the C-terminus intracellularly, there are some observations which indicate that this domain is not simply accessible to attempted perturbations made intracellularly, outside the lipid bilayer. For example, the lack of an effect of intracellular trypsin or pronase treatment on OHC and transfected cell NLC indicates that prestin's termini are somehow protected [7–9,28]. We would therefore expect that deletion of either the C- or N-terminus would abolish NLC, a view that has been confirmed by mutational analysis (see Fig. 1); [17,29]. Interestingly, in channel forming bacterial colicins an intracellular hydrophilic group of residues (or even larger appended tags) can be moved across the membrane in response to changes in voltage [10,11], a mechanism that could also operate in prestin since these charged clusters may be constrained close to the PM within the restricted sub-plasmalemmal space bounded by the subsurface cisternae. Indeed, this type of mechanism that colicin employs has been offered as a possible mechanism to account for area changes evoked by prestin activation [23]. Thus, we have no direct empiric evidence that the C-terminus of prestin is statically placed outside the bilayer. Nevertheless, our current work bears on this issue, since mutating charged residues in prestin that do not reside within the membrane field should not directly alter unitary charge movement. We found with our charge reversal mutations that, in no case, was the unitary charge of prestin's voltage altered, implying that these residues lie outside the membrane field. However, clear effects on voltage sensing were observed, with three mutations, *a*, *b* and *R571D* showing significant changes in V_h. We interpreted these results to indicate a shift in the steady state energy profile of the protein. Since both mutations of *cluster a* and *b* (which have opposite charge) shift V_h in the same direction, it is possible that simultaneous mutations of both could produce an augmented shift. Additionally, one mutant (charge *cluster a* that is most proximal to the membrane) shows a significant decrease in the total charge moved. We interpret this to mean that the number of functional motors in this mutant has decreased. This view is additionally supported by similar levels of surface targeting of prestin determined by FACS in cells transfected with this mutant compared to normal prestin. Moreover, this observation is also in line with our previous work on truncations at the most distal section of the C-terminus, where the number of functional motors within the membrane decreased as stop codons were successively placed within the residue range of 715 to 710. Truncations at residues more proximal to 710 produced non-functional motors despite proper membrane targeting. We additionally showed in that work that homo-multimerization occurs among prestin molecules, and

hypothesized that obligate interactions underlie prestin's motive force. It may be that our charge reversals also interfere with interactions of other proteins at the C-terminus.

One other possibility arises. It is known that Cl^- interactions with intracellular moieties of prestin are crucial for prestin function, and we have proposed that, in contrast to models suggesting extrinsic voltage sensing by Cl^-, Cl^- serves as an allosteric modulator of prestin. For this reason, it may be that anions might interact with the C-terminal charge clusters, at least with those two clusters which reside most proximal to the membrane (*clusters a, b*), since only those showed substantial shifts in voltage sensing. Recently, manipulation of the STAS domain, which is conserved within the C-terminus among SLC26 transporter family members has been shown to inhibit sulfate transport in SULTR1.2 [19]. This was observed in the presence of normal membrane targeting. We are currently investigating whether our charge reversal mutants alter multimerization and Cl^- sensitivity in prestin.

In sum, we hypothesize that the C-terminal charged clusters of prestin, while not interacting with the membrane field to alter unitary charge movements in prestin, may work by intracellular interactions with either other proteins or anions, namely via allosteric means.

Acknowledgements

Support was provided by NIH NIDCD grants DC 000273 (JSS) and K08 (DN). We thank Peter Dallos and colleagues for the gerbil prestin clone, and Margaret Mazzucco for technical help.

References

[1] L. Aravind, E.V. Koonin, The STAS domain—a link between anion transporters and antisigma-factor antagonists, Curr. Biol. 10 (2000) R53–R55.
[2] J.F. Ashmore, A fast motile response in guinea-pig outer hair cells: the cellular basis of the cochlear amplifier, J. Physiol. (Lond.) 388 (1987) 323–347.
[3] J.F. Ashmore, Forward and reverse transduction in the mammalian cochlea, Neurosci. Res. 12 (Suppl.) (1990) S39–S50.
[4] I.A. Belyantseva, H.J. Adler, R. Curi, G.I. Frolenkov, B. Kachar, Expression and localization of prestin and the sugar transporter GLUT-5 during development of electromotility in cochlear outer hair cells, J. Neurosci. 20 (2000) RC116.
[5] W.E. Brownell, C.R. Bader, D. Bertrand, Y. de Ribaupierre, Evoked mechanical responses of isolated cochlear outer hair cells, Science 227 (1985) 194–196.
[6] L. Deak, J. Zheng, A. Orem, G.G. Du, S. Aguinaga, K. Matsuda, P. Dallos, Effects of cyclic nucleoticles on the function of prestin, J. Physiol.-Lond. 563 (2005) 483–496.
[7] X.X. Dong, K.H. Iwasa, Tension sensitivity of prestin: comparison with the membrane motor in outer hair cells, Biophys. J. 86 (2004) 1201–1208.
[8] G. Huang, J. Santos-Sacchi, Motility voltage sensor of the outer hair cell resides within the lateral plasma membrane, Proc. Natl. Acad. Sci. USA 91 (1994) 12268–12272.
[9] S. Kakehata, J. Santos-Sacchi, Membrane tension directly shifts voltage dependence of outer hair cell motility and associated gating charge, Biophys. J. 68 (1995) 2190–2197.
[10] P.K. Kienker, K.S. Jakes, R.O. Blaustein, C. Miller, A. Finkelstein, Sizing the protein translocation pathway of colicin Ia channels, J. Gen. Physiol. 122 (2003) 161–176.
[11] P.K. Kienker, X. Qiu, S.L. Slatin, A. Finkelstein, K.S. Jakes, Transmembrane insertion of the colicin Ia hydrophobic hairpin, J. Membr. Biol. 157 (1997) 27–37.
[12] M.C. Liberman, J. Gao, D.Z. He, X. Wu, S. Jia, J. Zuo, Prestin is required for electromotility of the outer hair cell and for the cochlear amplifier, Nature 419 (2002) 300–304.
[13] H. Lohi, M. Kujala, E. Kerkela, U. Saarialho-Kere, M. Kestila, J. Kere, Mapping of five new putative anion transporter genes in human and characterization of SLC26A6, a candidate gene for pancreatic anion exchanger, Genomics 70 (2000) 102–112.
[14] H. Lohi, M. Kujala, S. Makela, E. Lehtonen, M. Kestila, U. Saarialho-Kere, D. Markovich, J. Kere, Functional characterization of three novel tissue-specific anion exchangers SLC26A7, -A8, and -A9, J. Biol. Chem. 277 (2002) 14246–14254.
[15] J. Ludwig, D. Oliver, G. Frank, N. Klocker, A.W. Gummer, B. Fakler, Reciprocal electromechanical properties of rat prestin: the motor molecule from rat outer hair cells, Proc. Natl. Acad. Sci. USA 98 (2001) 4178–4183.
[16] K. Matsuda, J. Zheng, G.-G. Du, L. Deak, E. Navarrete, P. Dallos, Protein kinase C and voltage-dependent capacitance in prestin-transfected TSA cells, Assoc. Res. Otolaryngol. Abs. (2003) 105.
[17] D.S. Navaratnam, J.-P. Bai, H. Samaranayake, J. Santos-Sacchi, N-terminal mediated homo-multimerization of prestin, the outer hair cell motor protein, Biophys. J. 89 (2005) 3345–3352.
[18] D. Oliver, D.Z. He, N. Klocker, J. Ludwig, U. Schulte, S. Waldegger, J.P. Ruppersberg, P. Dallos, B. Fakler, Intracellular anions as the voltage sensor of prestin, the outer hair cell motor protein, Science 292 (2001) 2340–2343.
[19] H. Rouached, P. Berthomieu, E. El Kassis, N. Cathala, V. Catherinot, G. Labesse, J.C. Davidian, P. Fourcroy, Structural functional analysis of the C-terminal STAS (sulfate transporter and anti-sigma antagonist) domain of the Arabidopsis thaliana sulfate transporter SULTR1.2, J. Biol. Chem. 280 (2005) 15976–15983.
[20] V. Rybalchenko, J. Santos-Sacchi, Cl- flux through a non-selective, stretch-sensitive conductance influences the outer hair cell motor of the guinea-pig, J. Physiol. 547 (2003) 873–891.
[21] J. Santos-Sacchi, J.P. Dilger, Whole cell currents and mechanical responses of isolated outer hair cells, Hear. Res. 35 (1988) 143–150.
[22] J. Santos-Sacchi, S. Kakehata, S. Takahashi, Effects of membrane potential on the voltage dependence of motility-related charge in outer hair cells of the guinea-pig, J. Physiol. 510 (Pt 1) (1998) 225–235.
[23] J. Santos-Sacchi, E. Navarrete, Voltage-dependent changes in specific membrane capacitance caused by prestin, the outer hair cell lateral membrane motor, Pflugers Arch. 444 (2002) 99–106.
[24] J. Santos-Sacchi, New tunes from Corti's organ: the outer hair cell boogie rules, Curr. Opin. Neurobiol. 13 (2003) 459–468.
[25] J. Santos-Sacchi, Reversible inhibition of voltage-dependent outer hair cell motility and capacitance, J. Neurosci. 11 (1991) 3096–3110.
[26] J. Santos-Sacchi, W.X. Shen, J. Zheng, P. Dallos, Effects of membrane potential and tension on prestin, the outer hair cell lateral membrane motor protein, J. Physiol.-Lond. 531 (2001) 661–666.
[27] L. Song, A. Seeger, J. Santos-Sacchi, On membrane motor activity and chloride flux in the outer hair cell: Lessons learned from the environmental toxin tributyltin, Biophys. J. 88 (2005) 2350–2362.
[28] S. Takahashi, J. Santos-Sacchi, Non-uniform mapping of stress-induced, motility-related charge movement in the outer hair cell plasma membrane, Pflugers Arch. 441 (2001) 506–513.
[29] J. Zheng, G.G. Du, K. Matsuda, A. Orem, S. Aguinaga, L. Deak, E. Navarrete, L.D. Madison, P. Dallos, The C-terminus of prestin influences nonlinear capacitance and plasma membrane targeting, J. Cell Sci. 118 (2005) 2987–2996.
[30] J. Zheng, K.B. Long, W. Shen, L.D. Madison, P. Dallos, Prestin topology: localization of protein epitopes in relation to the plasma membrane, Neuroreport 12 (2001) 1929–1935.
[31] J. Zheng, W. Shen, D. He, K. Long, L. Madison, P. Dallos, Prestin is the motor protein of cochlear outer hair cells, Nature 405 (2000) 149–155.